REAL-TIME WAVE DIGITAL SIMULATION OF CASCADED VACUUM TUBE AMPLIFIERS USING MODIFIED BLOCKWISE METHOD

Jingjie Zhang, Julius O. Smith III

Center for Computer Research in Music and Acoustics (CCRMA), Stanford University
660 Lomita Drive, Stanford, CA 94305, USA
[jingjiez|jos]@ccrma.stanford.edu

ABSTRACT

Vacuum tube amplifiers, known for their acclaimed distortion characteristics, are still widely used in hi-fi audio devices. However, bulky, fragile and power-consuming vacuum tube devices have also motivated much research on digital emulation of vacuum tube amplifier behaviors. Recent studies on Wave Digital Filters (WDF) have made possible the modeling of multi-stage vacuum tube amplifiers within single WDF SPQR trees. Our research combines the latest progress on WDF with the modified blockwise method to reduce the overall computational complexity of modeling cascaded vacuum tube amplifiers by decomposing the whole circuit into several small stages containing only two adjacent triodes. Certain performance optimization methods are discussed and applied in the eventual real-time implementation.

1. INTRODUCTION

Having been displaced by semiconductor technologies in almost all areas of electronics, vacuum tube circuits are still widely used in hi-fi audio amplifiers and high-end guitar amplifiers due to the unique harmonic distortion characteristics produced by overdriven tubes that are preferred by human ears. On the other hand, driven by certain shortcomings of vacuum tube devices, such as large size and weight, poor durability and high power consumption, digital simulation of the behaviors of vacuum tube amplifiers, especially tube guitar amplifiers, has been an emerging research topic since the mid-1990s. In [1], Pakarinen and Yeh reviewed several digital techniques that emulate vacuum tube guitar amplifier behaviors.

Introduced by Fettweis, Wave Digital Filters (WDF) [2] are a class of digital filters that mimic classical filter structures, preferably lattice or ladder structures, by utilizing a wave-variable representation. Because of their superior numerical properties and stability under finite-arithmetic conditions, WDF have been successfully applied in digital modeling of lumped electronic or physical systems over the past few decades, as these systems can be typically represented by a set of blocks connected with each other through electrical or physical ports. It is thus reasonable that in recent years WDF have become widely applied in the field of nonlinear audio system modeling as a solid approach.

Digital modeling using classical WDF is able to handle series and parallel circuits containing a single-port delay-free nonlinearity. Reflection-free ports [3] are introduced to resolve the delay-free loop created by port connections, and a single-port nonlinearity [4] can be accommodated in a binary connection tree [5, 6]. However, the mathematical model of a vacuum tube triode is usually a dual-port or triple-port delay-free module. Moreover, circuits containing vacuum tube triodes usually cannot be simply decomposed into series and parallel topologies due to the feedback around the ports. Previous practices [7, 8, 9, 10] broke the multiple delay-free loops within WDF triode and JFET models by means of ad hoc unit delays, at the cost of accuracy and even stability.

Recently, Werner *et al.* [11, 12, 13, 14] extended the classical WDF adaptors to include the $\mathcal{R}$(Rigid)-type adaptor, a wave-domain scattering matrix [15] formed by a general approach based on Modified Nodal Analysis (MNA) [16] that resolves both arbitrary complex topologies [17] and multiple/multiport nonlinearities. The K-method [18] was used to resolve the multiple delay-free loops within these nonlinearities and thus make them tractable through tabulation. However, multidimensional tabulation often results in high memory-space consumption. Hence, while 1D nonlinearities are easily handled by linearly interpolated lookup tables [19], piecewise polynomial interpolation [20] or canonical piecewise-linear representation [4, 21], multidimensional iterative techniques [22] are typically used as an alternative to the tabulation approach when there are several interacting nonlinearities. Extending the previous binary connection tree containing three-port WDF adaptors, the $\mathcal{R}$-type adaptor has led to a new tree structure—an SPQR tree [17], which is able to absorb multiple nonlinearities into one single tree. Such a strategy was taken in [23] to simulate a multi-stage tube guitar amplifier, whereas it still remains to be improved for the sake of real-time capability, due to the dramatically increasing complexity of solving multidimensional nonlinear equations as the dimension increases. Although recent works on system identification and gray-box modeling techniques by Eichas *et al.* [24] are capable of modeling nonlinear guitar amplifiers with relatively low computational load, they are not based on the knowledge of the circuits and hence, cannot exactly model the behavior of the knobs in amplifiers.

In this paper, a certain type of vacuum tube amplifier circuit—cascaded vacuum tube amplifiers—are of concern, since a large proportion of vacuum tube amplifiers, especially vacuum tube guitar preamplifiers, appear to have a cascading structure. Previous studies done by Mačák [25, 26, 27, 28] introduced a modified blockwise method, which decomposes cascaded vacuum tube amplifiers properly into separate small stages to keep low the dimension of the local nonlinear system to be numerically solved each time and therefore, reduce the overall computational complexity of the whole simulation without affecting the mutual interactions between adjacent amplifier circuits. Similar strategy was also devised in [29] where two stages of the TR-808 bass drum were carefully separated. As a demonstration of combining WDF modeling techniques with the modified blockwise method, a case study of a vacuum tube guitar preamplifier in cascading structure is presented. Performance optimization methods that contribute to the real-time behavior of the eventual implementation are discussed, as well as simulation results.

This work was supported by Stanford Art Institute 2017-18 Fellowship

The remainder of this paper is structured as follows: Section 2 reviews the previous research on resolving multiple/multiport WDF nonlinearities within a single SPQR tree. Section 3 illuminates the details of the modified blockwise method and its significance to the modeling of cascaded vacuum tube amplifiers. The case study is given in Section 4. Section 5 summarizes the results and discusses future research directions.

2. PREVIOUS WORK

In this Section, recent developments in WDF modeling of nonlinear circuits are reviewed. In particular, two approaches that resolve the multiple delay-free loops within multiple/multiport nonlinearities within $\mathcal{R}$-type adaptors are discussed.

Previous studies [14, 17] have developed a general approach that can decompose any given circuit into **S**eries, **P**arallel, and **R**igidly connected WDF elements, and thus form a WDF SPQR tree, which uses an $\mathcal{R}$-type adaptor to absorb any complex (neither series nor parallel) topologies. All nonlinearities are placed at the "roots" of the SPQR tree, while the remaining subtrees containing series, parallel, or even other R-type connected linear elements can be modeled using conventional WDF theory. Thévenin port equivalents and Modified Nodal Analysis (MNA) [16] are utilized to compute the wave scattering matrix $\mathbf{S}$ for each $\mathcal{R}$-type adaptor:

$$\begin{bmatrix}\mathbf{b}_I\\ \mathbf{b}_E\end{bmatrix} = \mathbf{S}\begin{bmatrix}\mathbf{a}_I\\ \mathbf{a}_E\end{bmatrix} = \begin{bmatrix}\mathbf{S}_{11} & \mathbf{S}_{12}\\ \mathbf{S}_{21} & \mathbf{S}_{22}\end{bmatrix}\begin{bmatrix}\mathbf{a}_I\\ \mathbf{a}_E\end{bmatrix}, \tag{1}$$

where $\mathbf{a}_I$ and $\mathbf{b}_I$ represent the vectors of internal incident and reflected waves from the nonlinearities, while $\mathbf{a}_E$ and $\mathbf{b}_E$ represent the external incident and reflected waves from the subtrees.

Whereas the wave domain nonlinear relationship between $\mathbf{a}_I$ and $\mathbf{b}_I$ can be represented by $\mathbf{a}_I = F_w(\mathbf{b}_I)$, it is much easier to obtain the Kirchhoff domain nonlinear relationship:

$$\mathbf{i}_C = F_k(\mathbf{v}_C), \tag{2}$$

since the behaviors of most nonlinear electronic devices are usually defined in the Kirchhoff domain, while only some specific nonlinearities can be modeled in wave domain using the Lambert $\mathcal{W}$ function [30, 31, 32].

Therefore, the internal wave vectors $\mathbf{a}_I$ and $\mathbf{b}_I$ are converted to the corresponding Kirchhoff vectors $\mathbf{i}_C$ and $\mathbf{v}_C$ using a w–K converter matrix $\mathbf{C}$:

$$\begin{bmatrix}\mathbf{v}_C\\ \mathbf{a}_I\end{bmatrix} = \begin{bmatrix}\mathbf{C}_{11} & \mathbf{C}_{12}\\ \mathbf{C}_{21} & \mathbf{C}_{22}\end{bmatrix}\begin{bmatrix}\mathbf{i}_C\\ \mathbf{b}_I\end{bmatrix} = \begin{bmatrix}-\mathbf{R}_I & \mathbf{I}\\ -2\mathbf{R}_I & \mathbf{I}\end{bmatrix}\begin{bmatrix}\mathbf{i}_C\\ \mathbf{b}_I\end{bmatrix}, \tag{3}$$

where $\mathbf{R}_I$ is a diagonal matrix of internal port resistances. Combining (1) and (3) yields a new scattering relationship:

$$\begin{bmatrix}\mathbf{v}_C\\ \mathbf{b}_E\end{bmatrix} = \begin{bmatrix}\mathbf{F} & \mathbf{E}\\ \mathbf{N} & \mathbf{M}\end{bmatrix}\begin{bmatrix}\mathbf{i}_C\\ \mathbf{a}_E\end{bmatrix}, \tag{4}$$

where

$$\begin{cases}\mathbf{E} = \mathbf{C}_{12}(\mathbf{I} + \mathbf{S}_{11}\mathbf{H}\mathbf{C}_{22})\mathbf{S}_{12}\\ \mathbf{F} = \mathbf{C}_{12}\mathbf{S}_{11}\mathbf{H}\mathbf{C}_{21} + \mathbf{C}_{11}\\ \mathbf{M} = \mathbf{S}_{21}\mathbf{H}\mathbf{C}_{22}\mathbf{S}_{12} + \mathbf{S}_{22}\\ \mathbf{N} = \mathbf{S}_{21}\mathbf{H}\mathbf{C}_{21},\end{cases} \tag{5}$$

with $\mathbf{H} = (\mathbf{I} - \mathbf{C}_{22}\mathbf{S}_{11})^{-1}$.

Plugging (2) into (4) yields the delay-free loops within the $\mathcal{R}$-type adaptor:

$$\mathbf{v}_C = \mathbf{E}\mathbf{a}_E + \mathbf{F}F_k(\mathbf{v}_C). \tag{6}$$

The delay-free loops in (6) can be resolved using either K-method or iterative techniques. In terms of high speed data access and memory consumption, using multidimensional tables transformed by K-method [12, 18] in real-time simulation becomes more expensive as the dimension increases. In addition, the neighbor searching and scattered interpolation of multidimensional table data further aggravates the computational load. As a more general approach, multidimensional iterative techniques solve instantaneous loops by finding numerical solutions to the given nonlinear systems, and hence are applied in [22] to offer an alternative to K-method. To solve for $\mathbf{v}_C$ in (6), the following multidimensional nonlinear equation can be constructed:

$$H(\mathbf{v}_C) = \mathbf{E}\mathbf{a}_E + \mathbf{F}F_k(\mathbf{v}_C) - \mathbf{v}_C = 0. \tag{7}$$

Several iterative approaches are available to obtain the numerical solution to this equation. The simplest and typically most effective way is multidimensional Newton's method. For the multidimensional function $H(\mathbf{v}_C)$, given an initial guess $\mathbf{v}_C^0$ in a sufficiently close neighborhood of one of its zeros, a numerical approximation of the solution can be obtained iteratively by

$$\mathbf{v}_C^{k+1} = \mathbf{v}_C^k - J_H(\mathbf{v}_C^k)^{-1}H(\mathbf{v}_C^k), \tag{8}$$

where J_H is the Jacobian matrix of H. The choice of the initial guess $\mathbf{v}_C^0$ is detailed in [22]. Although several advanced iterative algorithms based on Newton's method can be devised to achieve a higher convergence rate, the overall computational complexity within each iteration expands dramatically as the dimension of the inverse Jacobian matrix J_H^{-1} increases, especially in [23] where four WDF triode models were involved in one single SPQR tree.

3. MODIFIED BLOCKWISE METHOD

As discussed in the previous section, performance degradation in high-dimensional cases is dramatic in the multi-nonlinearity WDF systems resolved by either K-method or iterative methods, while such circumstances are inevitable when cascaded vacuum tube amplifiers are modeled as a whole. On the other hand, as a common approach to deal with complex cascaded systems, simply decomposing cascaded tube amplifiers into minimal separate stages (*i.e.*, one tube per stage) is also not applicable due to the strong mutual interactions that comes from the loading effect between two adjacent tube amplifiers, although it minimizes the dimension of the local nonlinear equations to be solved each time.

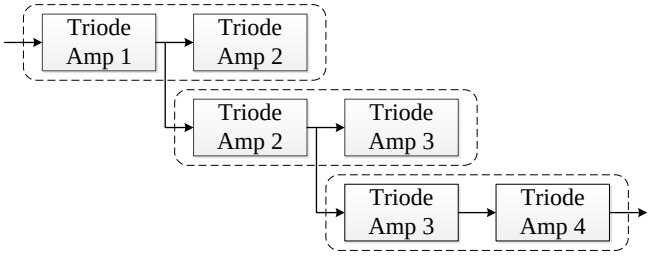

Figure 1: *Decomposing cascaded vacuum tube amplifiers using the modified blockwise method.*

In [28], the loading effects between three cascaded typical common-cathode triode amplifiers have been measured and compared. It has been proved that there is very small interaction between the first and the third amplifier and hence, it is sufficient to consider only the second amplifier as the nonlinear load for the first one, which lays the foundation of the modified blockwise method. Applied in several previous practices [25, 26, 27] on equation-based simulation of cascaded vacuum tube amplifiers, the modified blockwise method decomposes the cascaded amplifiers into several coupled triode amplifier stages that are modeled separately as illustrated in Fig. 1. It is noteworthy that the extra computational load introduced by the redundant triode amplifiers involved in the simulation is far outweighed by the reduced overall computational complexity of the whole system.

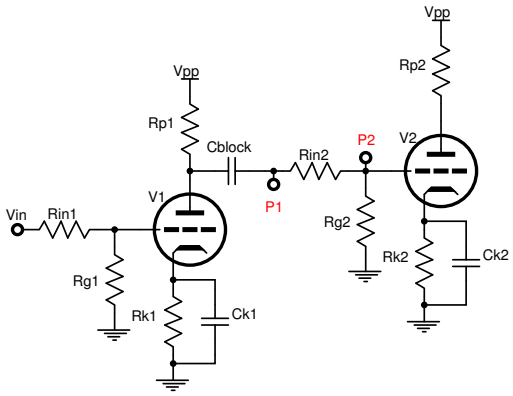

Figure 2: *Extracting the proper output signal of the first amplifier in a coupled common-cathode triode amplifier stage.*

The modified blockwise structure ensures that in each stage, the nonlinear current flowing into the grid of the second triode is taken into account and therefore, the output signal of the first triode amplifier is correct and ready to be fed into the next stage. Fig. 2 points out the circuit node P_1 where the output signal of the first amplifier is usually extracted in a coupled common-cathode triode amplifier stage. On the other hand, extracting the signal at P_2 is usually not applicable, although it cuts down the number of redundant components in the next stage. Such a conclusion is drawn on the basis of the triodes' grid limiting behavior [33] illustrated in Fig. 3. As the input voltage V_{in} to the triode amplifier is made larger, the grid current I_g increases, causing an increased voltage drop across the grid resistor R_{in}. This tends to make the grid voltage V_g increase much less than the input. As a result, the grid resistor R_{in} is of great significance and hence cannot be simply separated from the simulation unless the triode's operating point is not located in the grid limiting region under any circumstances.

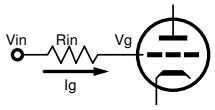

Figure 3: *Grid limiting behavior of a vacuum tube triode.*

4. CASE STUDY

As an example of combining multi-nonlinearity WDF modeling techniques with the modified blockwise method, we study the preamplifier stage of the MESA/Boogie® Mark II-B™ guitar amplifier, which consists of five cascaded vacuum tube triode amplifiers. The prototype of this circuit was patented by Smith [34] in 1980 as the world's first high gain dual mode channel switching amplifier.

4.1. System Decomposition

As shown in Fig. 5a and 5b, both "Clean" and "Lead" branches are cascaded vacuum tube triode amplifiers that can be decomposed into small coupled triode amplifier stages using the modified blockwise method. The circuit nodes where signals should be extracted are marked in these schematics. In Fig. 5a, the output signal of *Stage* 3 is extracted at P_2 rather than the node between capacitor C_8 and resistor R_4 simply because it is much easier to get the plate voltage of triode V1B in the corresponding WDF SPQR tree as presented in Fig. 6; whereas extracting signal elsewhere requires extra subtraction. It is also worth mentioning that the circuit node P_3 in both Fig. 5a and 5b is carefully chosen so that the "Lead" and "Clean" branches can share the same coupled triode output stage without extra computational load. Such a strategy is based on careful measurements of the input and output signals of *Stage* 5, a cathode follower which has no gain but a constant grid-to-cathode voltage.

On the basis of the marked circuit nodes in Fig. 5, the reference circuit is decomposed into five coupled triode amplifier stages organized in the modified blockwise structure and then modeled using WDF techniques. Fig. 6 shows the resulting SPQR trees of each stage and a diagram of the system structure at the top right corner that illustrates the relationship between the dual triode stages in the modified blockwise structure and the original cascaded circuit stages, where the original stages containing triodes are marked with a darker color. All the linear elements in the circuits are modeled using voltage wave variables. The active sections of a potentiometer are treated separately and identified by suffix numbers (*e.g.*, the potentiometer "Volume" in *Stage* 3 is separated into "Vol1" and "Vol2").

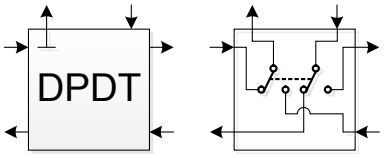

Figure 4: *Internal structure of a wave-domain double-point, double-throw (DPDT) switch.*

In previous WDF modeling practices [29, 35], the single-pole, single-throw (SPST) switch are usually modeled as non-adaptable elements at the root of the trees. In this work, a wave-domain double-point, double-throw (DPDT) switch is devised to model the equivalent behavior of some circuits containing SPST switches. The common port of a DPDT switch can only be connected with one of the two sub-ports, as illustrated in Fig. 4. The two different states of an SPST switch in a circuit will result in two different local topologies. If the differences are within one subtree of an $\mathcal{R}$-type adaptor, then this wave-domain DPDT switch can be utilized to adapt the two local subtrees derived from the two topolo-

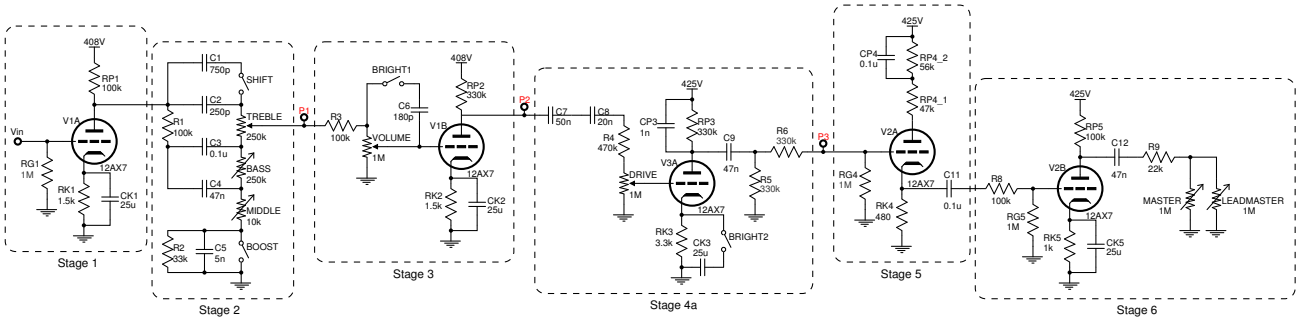

(a) *"Lead" mode*

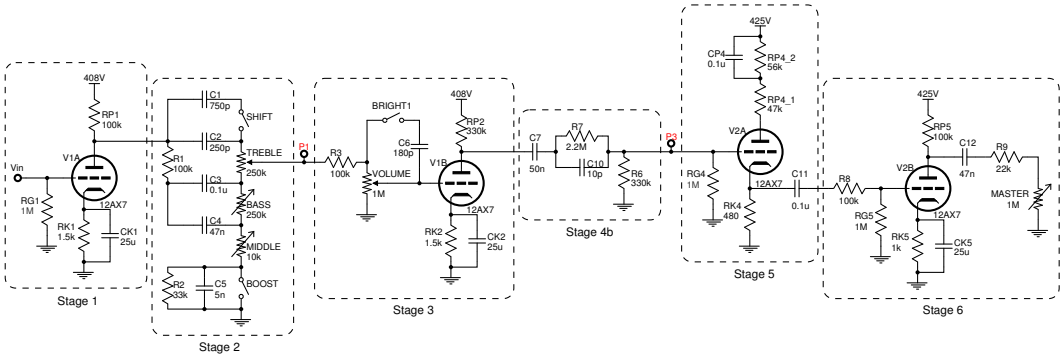

(b) *"Clean" mode*

Figure 5: *Schematic of MESA/Boogie® Mark II-B™ guitar preamplifier in both "Lead" and "Clean" modes.*

gies. In the process, some elements will inevitably appear twice in the whole SPQR tree, therefore, the two identical elements are distinguished from each other by an extra apostrophe in the labels (*e.g.*, the potentiometer "Middle" in *Stage* 2 has two identical WDF models "M" and "M′" in two local subtrees).

4.2. Resolving Coupled Triodes

Although the modified blockwise decomposition of the reference circuit reduces the dimension of the local nonlinear system from 8D/10D to 4D (coupled triode amplifiers), the size of a K-method-transformed multidimensional lookup table is still too large for real-time simulations. Thus, in this case study, multidimensional Newton's method is used to resolve the dual triodes within one SPQR tree, which involves utilizing the Jacobian matrix J as a direction to find the root of the nonlinear equations (7) formed by the mathematical models of these triodes. However, previous triode models [36, 37, 38, 39] are all piece-wise nonlinear functions that result in poor performance near the points of discontinuity.

Preferred by recent research [23, 28, 40, 41], the physically-motivated Dempwolf triode model [42] smooths the discontinuity by combinations of exponential and logarithmic functions:

$$\begin{cases} I_{gk} = f(V_{gk}) = G_g \cdot (\frac{1}{C_g}\log(1+e^{C_g \cdot V_{gk}}))^{\xi} + I_{g0} \\ I_k = g(V_{gk}, V_{pk}) = G \cdot (\frac{1}{C}\log(1+e^{C\cdot(\frac{V_{pk}}{\mu}+V_{gk})}))^{\gamma} \\ I_{pk} = I_k - I_{gk} = g(V_{gk}, V_{pk}) - f(V_{gk}), \end{cases} \quad (9)$$

Table 1: *Dempwolf triode model parameters of a 12AX7 tube.*

G_g	C_g	ξ	I_{g0}
6.177E-4	9.901	1.314	8.025E-8
G	C	γ	μ
2.242E-3	3.4	1.26	103.2

with grid-to-cathode voltage and current V_{gk}, I_{gk}, plate-to-cathode voltage and current V_{pk}, I_{pk}, cathode current I_k, and constant model parameters such as perveances G_g, G, adaption factors C_g, C and exponents ξ, γ. For a typical **12AX7** tube, the model parameters are given in Table 1.

For dual triode amplifier stages, plugging (9) into (2) yields

$$\mathbf{i}_C = \begin{bmatrix} I_{gk1} \\ I_{pk1} \\ I_{gk2} \\ I_{pk2} \end{bmatrix} = F_k(\mathbf{v}_C) = F_k(\begin{bmatrix} V_{gk1} \\ V_{pk1} \\ V_{gk2} \\ V_{pk2} \end{bmatrix}) = \begin{bmatrix} f_1 \\ g_1 - f_1 \\ f_2 \\ g_2 - f_2 \end{bmatrix}, \quad (10)$$

where f_i denotes $f(V_{gki})$ and g_i denotes $g(V_{gki}, V_{pki}) - f(V_{gki})$.

Hence, the multidimensional nonlinear equation (7) of each dual triode amplifier stage can be expressed as

$$H(\begin{bmatrix} V_{gk1} \\ V_{pk1} \\ V_{gk2} \\ V_{pk2} \end{bmatrix}) = \mathbf{E}\mathbf{a}_E + \mathbf{F}\begin{bmatrix} f_1 \\ g_1 - f_1 \\ f_2 \\ g_2 - f_2 \end{bmatrix} - \begin{bmatrix} V_{gk1} \\ V_{pk1} \\ V_{gk2} \\ V_{pk2} \end{bmatrix} = 0. \quad (11)$$

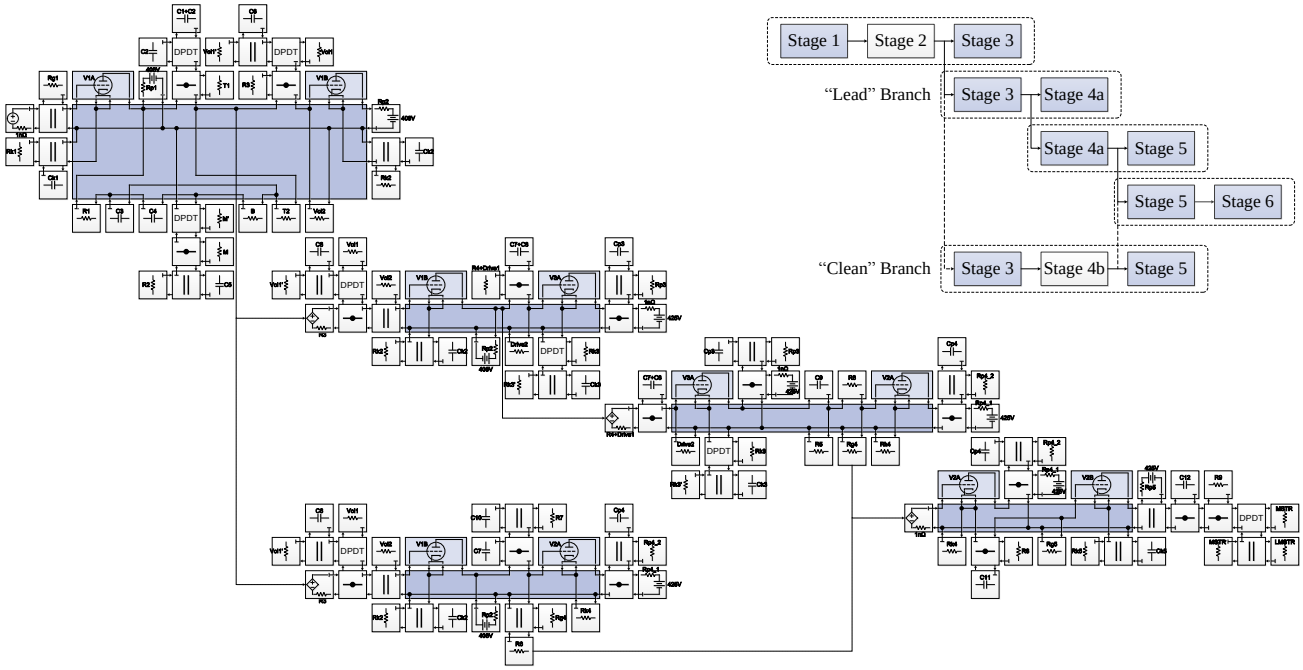

Figure 6: *Modified blockwise WDF model of MESA/Boogie® Mark II-B™ guitar preamplifier.*

The corresponding iteration expression (8) thus becomes

$$\begin{bmatrix} V_{gk1} \\ V_{pk1} \\ V_{gk2} \\ V_{pk2} \end{bmatrix}^{k+1} = \begin{bmatrix} V_{gk1} \\ V_{pk1} \\ V_{gk2} \\ V_{pk2} \end{bmatrix}^{k} - J_H\Big(\begin{bmatrix} V_{gk1} \\ V_{pk1} \\ V_{gk2} \\ V_{pk2} \end{bmatrix}^{k}\Big)^{-1} H\Big(\begin{bmatrix} V_{gk1} \\ V_{pk1} \\ V_{gk2} \\ V_{pk2} \end{bmatrix}^{k}\Big), \quad (12)$$

where the four-dimensional Jacobian matrix J_H is given by

$$J_H = \mathbf{F} J_{F_k} - \mathbf{I}, \quad (13)$$

with

$$J_{F_k} = \begin{bmatrix} \frac{\partial f_1}{\partial V_{gk1}} & 0 & 0 & 0 \\ \frac{\partial g_1}{\partial V_{gk1}} - \frac{\partial f_1}{\partial V_{gk1}} & \frac{\partial g_1}{\partial V_{pk1}} & 0 & 0 \\ 0 & 0 & \frac{\partial f_2}{\partial V_{gk2}} & 0 \\ 0 & 0 & \frac{\partial g_2}{\partial V_{gk2}} - \frac{\partial f_2}{\partial V_{gk2}} & \frac{\partial g_2}{\partial V_{pk2}} \end{bmatrix}. \quad (14)$$

4.3. Performance Optimization Methods

Various methods can be used to optimize the performance of the WDF simulation system to make it run in real time. A widely applied one is to tabulate the nonlinearity with a proper uniform interval and introduce linear interpolation into the table lookup process [19]. In this case study, the two nonlinear functions $I_{gk} = f(V_{gk})$ and $I_k = g(V_{gk}, V_{pk})$ in the Dempwolf triode model (9) are tabulated into two one-dimensional lookup tables corresponding to a pair of indices V_1, V_2 transformed through

$$\begin{bmatrix} V_1 \\ V_2 \end{bmatrix} = \begin{bmatrix} 1 & 0 \\ 1 & \frac{1}{\mu} \end{bmatrix} \begin{bmatrix} V_{gk} \\ V_{pk} \end{bmatrix}. \quad (15)$$

Combining (9) and (14) also yields

$$\frac{\partial g(V_{gk} + \frac{V_{pk}}{\mu})}{\partial V_{pk}} = \frac{1}{\mu} \frac{\partial g(V_{gk} + \frac{V_{pk}}{\mu})}{\partial V_{gk}}. \quad (16)$$

Thus, all the elements in the Jacobian matrix J_{F_k} (14) can also be covered by two 1D nonlinear tables $\frac{\partial f}{\partial V_{gk}}$ and $\frac{\partial g}{\partial V_{gk}}$ corresponding to the same pair of indices V_1, V_2 given in (15).

Linear interpolation is applied when utilizing the four 1D tables $f(V_1)$, $\frac{\partial f}{\partial V_{gk}}(V_1)$, $g(V_2)$, $\frac{\partial g}{\partial V_{gk}}(V_2)$. For a 1D table $y[n]$, given an accurate value x between two adjacent integer indices n and $n+1$, the linear interpolation result $y[x]$ is defined by

$$y[x] = y[n] + (x - n)(y[n+1] - y[n]), \quad (17)$$

which can be further optimized by introducing a different table $\Delta y[n] = y[n+1] - y[n]$ that replaces the extra subtraction:

$$y[x] = y[n] + (x - n)\Delta y[n] \quad (18)$$

Another approach to speed up the simulation process is developed from the perspective of matrix-operation performance tuning. In this study, the open source C++ linear algebra library Armadillo [43] is used to cover the basic matrix operations such as addition, multiplication and inversion. However, when solving the 4D local nonlinear system (11) within each coupled triode amplifier stage, the most time-consuming process in each iteration (12) is the inversion of the 4D matrix J_H, although the inversions of small matrices up to 4D are carried out explicitly inside Armadillo. This is due to the large overheads introduced by Armadillo wrappers to take different measures according to different matrix dimensions. The same situation occurs when Armadillo is calling the general matrix-vector multiplication (GEMV) in Basic Linear

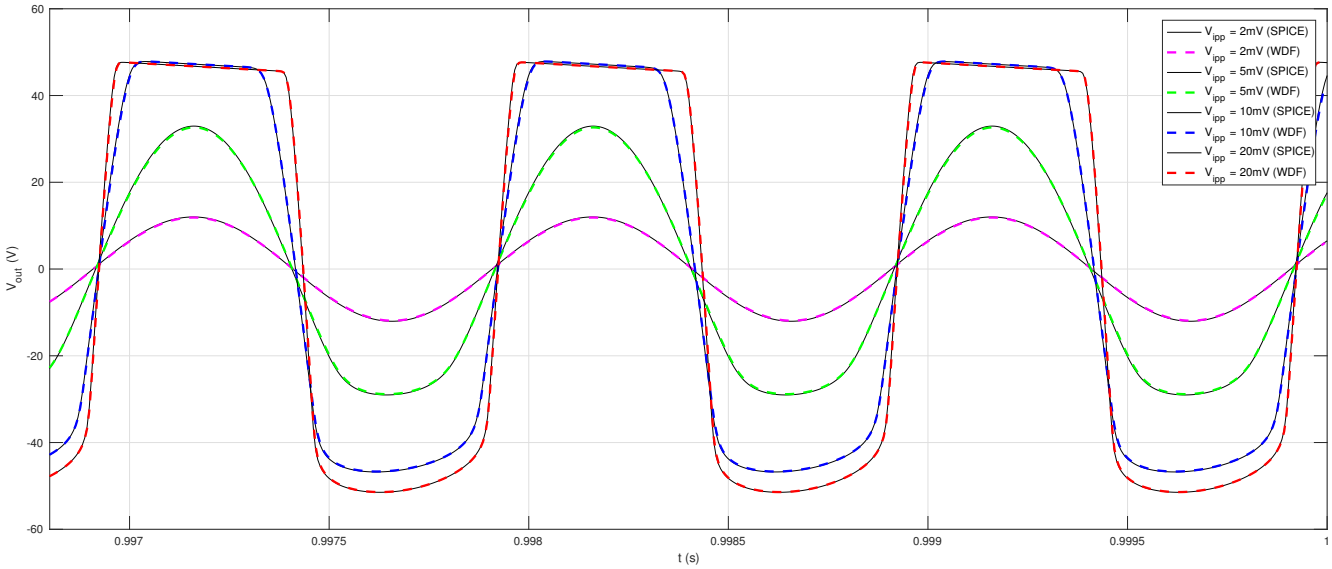

Figure 7: *Comparison of WDF and SPICE's time domain responses to different input signal levels.*

Algebra Subprograms (BLAS), in which case more overheads is introduced since BLAS is row-oriented so that an extra transposition is required when called by the column-oriented Armadillo. Therefore, explicit 4D matrix inversion and 4D matrix-vector multiplication are implemented to avoid extra overheads.

Finally, to further increase the simulation speed, a certain level of accuracy can be carefully sacrificed by increasing the error tolerance threshold TOL of the iterative root-finding process, which serves as a termination criterion for iteration:

$$||H(\mathbf{v}_C^k)|| \leq TOL \tag{19}$$

4.4. Simulation Results

The modified blockwise WDF system was implemented in C++ language and tested on a MacBook Pro with 2.3 GHz Intel Core i5 and 8GB RAM at 4x oversampling of a typical audio sampling rate of 44.1 kHz (176.4 kHz). After several successful initial offline behavioral tests, the system was tested in real-time with a buffer size of 256 samples and a 15.1% maximal CPU load.

To test the system's time domain response, 1kHz sinusoids with a small peak-to-peak voltage of 2mV, 5mV, 10mV and 20mV were used as input signal to observe in particular the transition from linear amplification to soft clipping in "Lead" mode. As presented in Fig. 7, the output waveforms of the WDF system show excellent agreement with LTspice simulation results of the same circuit. As the input amplitude increases gradually, the grid limiting first starts to appear in the negative cycle of the output waveform, and when the input level is even higher, the positive cycle is cut off. The error of a fully clipped output signal corresponding to a 1kHz, 250mV peak-to-peak input sinusoid is shown in Fig. 8. Most errors occur during zero-crossing with a maximum of 4.5V, which might be introduced by the alignment deviation after resampling SPICE results onto the time grid of the WDF simulation.

Fig. 9 shows the comparison of WDF and SPICE's frequency responses to a 1kHz, 250mV peak-to-peak input sinusoid. The SPICE results have been offset by 50Hz to create clarity. The first twenty harmonic peak frequencies of the WDF simulation

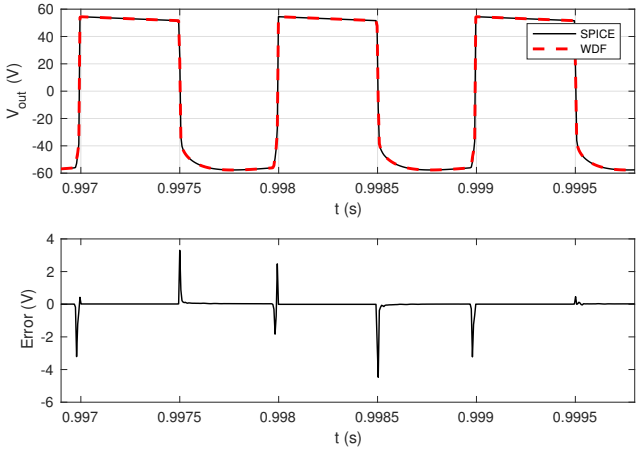

Figure 8: *Comparison of WDF and SPICE's time domain responses (top) and error (bottom) for a* 1*kHz,* 250*mV peak-to-peak input sinusoid.*

agree well with the SPICE results. To verify the system's behavior across the audible range, exponential sine sweeps [44] between 20Hz and 20kHz is used as input signal, the response spectrograms of "Clean" and "Lead" mode are presented in Fig. 10 and 11 respectively. It is confirmed that the harder clipping in "Lead" mode results in higher harmonics in the corresponding output signal.

Preserving a reasonably high accuracy of simulation, the modified blockwise WDF system shows superior performance advantages when compared with SPICE and single WDF SPQR tree system. For the "Lead" mode circuit containing five cascaded triode amplifiers, given a 1-second input sinusoid, the modified blockwise WDF system only spends around 370ms to finish the whole simulation, while a single WDF SPQR tree model of the same circuit requires more than 20s, and the corresponding simulation time of SPICE even exceeds 80s.

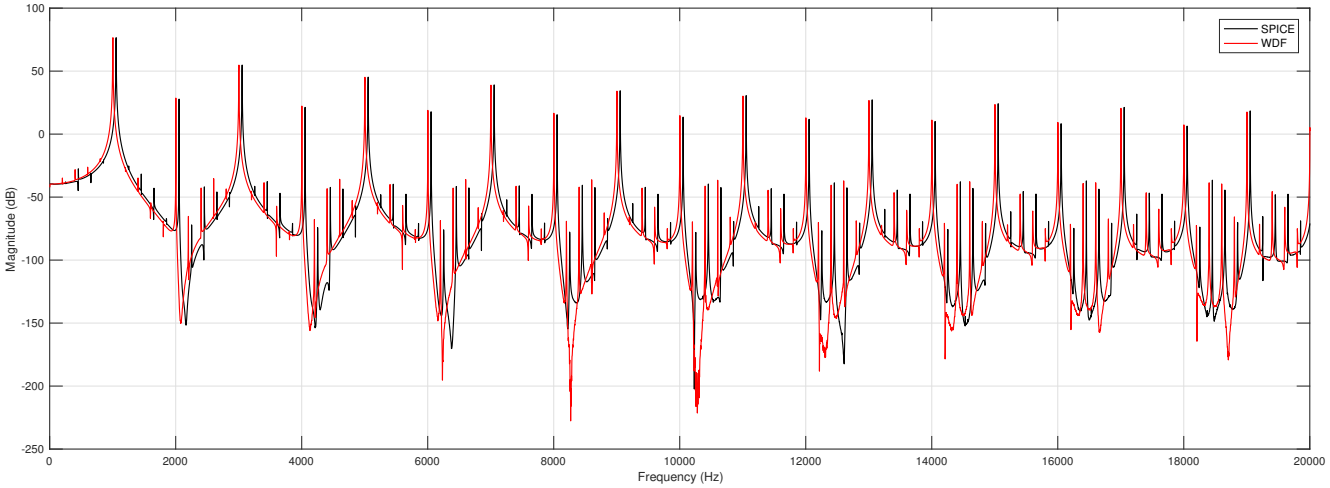

Figure 9: *Comparison of WDF and SPICE's frequency responses, a* 50*Hz offset is applied to SPICE result for intelligibility.*

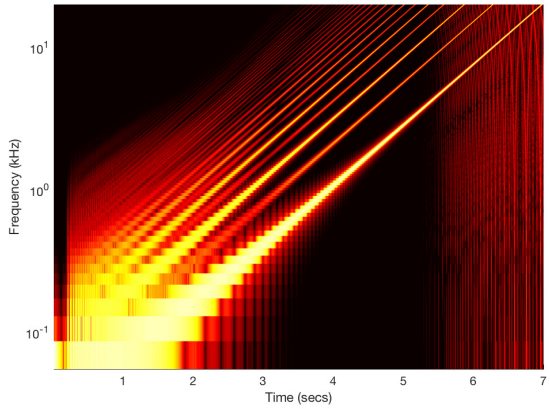

Figure 10: *Exponential sine sweep response spectrogram for* 20-20*kHz* 250*mV peak-to-peak input signals ("Clean" mode).*

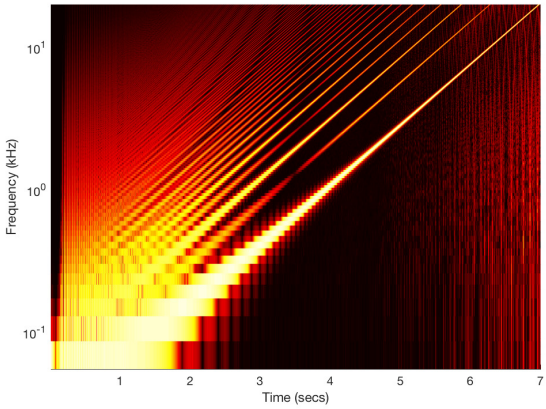

Figure 11: *Exponential sine sweep response spectrogram for* 20-20*kHz* 250*mV peak-to-peak input signals ("Lead" mode).*

5. CONCLUSION AND FUTURE WORK

In this paper, the modified blockwise method is applied to the WDF modeling of cascaded vacuum tube amplifiers to reduce the overall computational complexity of solving high-dimensional nonlinear systems. The cascaded tube amplifier was decomposed into several small stages containing two adjacent triodes. With the help of several performance optimization methods, such as lookup tables with linear interpolation and explicitly implemented matrix operations, the resulting modified blockwise WDF simulation system preserves a reasonably high precision in both time and frequency domains while exhibiting extremely high simulation speed on a standard laptop and hence, is capable of running in real-time.

As stated in the previous sections, the K-method transformed nonlinear multidimensional lookup tables are currently not competitive due to their high memory consumption and slow data-access speed. However, given enough memory, a table-lookup will be much faster than the iteration process. Sparse memory techniques [45] can be pursued, but they must ultimately be less expensive than Newton iterations. We therefore believe that future research could focus on 4D nonuniform tabulation, and high-speed 4D nearest neighbor searching algorithms. Unlike most vacuum tube preamplifiers in cascading structures, most vacuum tube power amplifiers are push-pull tube circuits that cannot be simulated by simply applying the strategies mentioned in this paper. Hence, further research can be done in this direction as well.

6. ACKNOWLEDGMENTS

Thanks to Brad Nelson and Steven R. Brill from the Stanford Computational Consulting (C^2) Service for helpful discussions on optimizing matrix-operation performance.

7. REFERENCES

[1] J. Pakarinen and D. T. Yeh, "A review of digital techniques for modeling vacuum-tube guitar amplifiers," *Comput. Music J.*, vol. 33, no. 2, pp. 85–100, 2009.

[2] A. Fettweis, "Wave digital filters: Theory and practice," *Proc. IEEE*, vol. 74, no. 2, pp. 270–327, Feb 1986.

[3] A. Fettweis and K. Meerkötter, "On adaptors for wave digital filters," *IEEE Trans. Acoust., Speech, Signal Process.*, vol. 23, no. 6, pp. 516–525, Dec 1975.

[4] K. Meerkötter and R. Scholtz, "Digital simulation of nonlinear circuits by wave digital filter principles," in *Proc. IEEE Intl. Symp. Circ. & Sys.*, Portland, OR, May 8–11, 1989, vol. 1, pp. 720–723.

[5] A. Sarti and G. De Sanctis, "Systematic methods for the implementation of nonlinear wave-digital structures," *IEEE Trans. Circuits Syst. I, Reg. Papers*, vol. 56, no. 2, pp. 460–472, Feb 2009.

[6] G. De Sanctis and A. Sarti, "Virtual analog modeling in the wave-digital domain," *IEEE Trans. Audio, Speech, Language Process.*, vol. 18, no. 4, pp. 715–727, May 2010.

[7] M. Karjalainen and J. Pakarinen, "Wave digital simulation of a vacuum-tube amplifier," in *Proc. IEEE Int. Conf. Acoust., Speech, Signal Process.*, Toulouse, France, May 15–19, 2006.

[8] J. Pakarinen, M. Tik, and M. Karjalainen, "Wave digital modeling of the output chain of a vacuum-tube amplifier," in *Proc. 12th Int. Conf. on Digital Audio Effects (DAFx-09)*, Como, Italy, Sep 1–4 2009.

[9] J. Pakarinen and M. Karjalainen, "Enhanced wave digital triode model for real-time tube amplifier emulation," *IEEE Trans. Audio, Speech, Language Process.*, vol. 18, no. 4, pp. 738–746, May 2010.

[10] D. Hernandez and J. Huang, "Emulation of junction field-effect transistors for real-time audio applications," *IEICE Electron. Express*, vol. 13, no. 12, pp. 1–11, 2016.

[11] K. J. Werner, J. O. Smith III, and J. S. Abel, "Wave digital filter adaptors for arbitrary topologies and multiport linear elements," in *Proc. 18th Int. Conf. on Digital Audio Effects (DAFx-15)*, Trondheim, Norway, Nov 30 – Dec 3, 2015.

[12] K. J. Werner, J. O. Smith III, and J. S. Abel, "Resolving wave digital filters with multiple/multiport nonlinearities," in *Proc. 18th Int. Conf. on Digital Audio Effects (DAFx-15)*, Trondheim, Norway, Nov 30 – Dec 3, 2015.

[13] K. J. Werner, V. Nangia, J. O. Smith III, and J. S. Abel, "A general and explicit formulation for wave digital filters with multiple/multiport nonlinearities and complicated topologies," in *Proc. IEEE Workshop Appl. Signal Process. Audio Acoust. (WASPAA)*, New Paltz, NY, Oct 18–21, 2015.

[14] K. J. Werner, A. Bernardini, J. O. Smith III, and A. Sarti, "Modeling circuits with arbitrary topologies and active linear multiports using wave digital filters," *IEEE Trans. Circuits Syst. I, Reg. Papers*, Jun 2018, In Press, DOI: https://doi.org/10.1109/TCSI.2018.2837912.

[15] V. Belevitch, *Classical network theory*, San Francisco, CA: Holden-Day, 1968.

[16] C.-W. Ho, A. Ruehli, and P. Brennan, "The modified nodal approach to network analysis," *IEEE Trans. Circuits and Syst.*, vol. 22, no. 6, pp. 504–509, Jun 1975.

[17] D. Fränken, J. Ochs, and K. Ochs, "Generation of wave digital structures for networks containing multiport elements," *IEEE Trans. Circuits Syst. I, Reg. Papers*, vol. 52, no. 3, pp. 586–596, Mar 2005.

[18] G. Borin, G. De Poli, and D. Rocchesso, "Elimination of delay-free loops in discrete-time models of nonlinear acoustic systems," *IEEE Trans. Speech Audio Process.*, vol. 8, pp. 597 – 605, Oct 2000.

[19] J. O. Smith III, "Efficient simulation of the reed-bore and bow-string mechanisms," in *Proc. Int. Comput. Music Conf.*, The Hague, The Netherlands, 1986, pp. 275–280.

[20] P. Cook and G. Scavone, *The synthesis toolkit in C++ (STK), version 4*, 2010. [Online]. Available: http://ccrma.stanford.edu/software/stk.

[21] A. Bernardini and A. Sarti, "Canonical piecewise-linear representation of curves in the wave digital domain," in *Proc. 25th Eur. Signal Process. Conf. (EUSIPCO)*, Kos, Greece, Aug 28–Sep 2, 2017, pp. 1125–1129.

[22] M. J. Olsen, K. J. Werner, and J. O. Smith III, "Resolving grouped nonlinearities in wave digital filters using iterative techniques," in *Proc. 19th Int. Conf. on Digital Audio Effects (DAFx-16)*, Brno, Czech Republic, Sep 5–9, 2016.

[23] W. R. Dunkel, M. Rest, K. J. Werner, M. J. Olsen, and J. O. Smith III, "The Fender Bassman 5F6-A family of preamplifier circuits—a wave digital filter case study," in *Proc. 19th Int. Conf. on Digital Audio Effects (DAFx-16)*, Brno, Czech Republic, Sep 5–9, 2016.

[24] F. Eichas, S. Möller, and U. Zölzer, "Block-oriented gray box modeling of guitar amplifiers," in *Proc. 20th Int. Conf. on Digital Audio Effects (DAFx-17)*, Edinburgh, UK, Sep 5–9, 2017, pp. 184–191.

[25] J. Mačák, "Modified blockwise method for simulation of guitar tube amplifiers," in *Proc. 33rd Int. Conf. on Telecom. and Signal Process. (TSP-10)*, Baden, Austria, Aug 17–20, 2010, pp. 1–4.

[26] J. Mačák and J. Schimmel, "Real-time guitar tube amplifier simulation using an approximation of differential equations," in *Proc. 13th Int. Conf. on Digital Audio Effects (DAFx-10)*, Graz, Austria, Sep 6–10, 2010.

[27] J. Mačák and J. Schimmel, "Real-time guitar preamp simulation using modified blockwise method and approximations," *EURASIP J. Adv. Signal Process.*, 2011, Article #629309.

[28] J. Mačák, *Real-time digital simulation of guitar amplifiers as audio effects*, Ph.D. thesis, Brno University of Technology, Brno, 2012.

[29] K. J. Werner, *Virtual analog modeling of audio circuitry using wave digital filters*, Ph.D. thesis, Stanford University, Stanford, CA, pp. 165–170, 2016.

[30] R. C. D. Paiva, S. D'Angelo, J. Pakarinen, and V. Valimaki, "Emulation of operational amplifiers and diodes in audio distortion circuits," *IEEE Trans. Circuits Syst. II, Exp. Briefs*, vol. 59, no. 10, pp. 688–692, Oct 2012.

[31] K. J. Werner, V. Nangia, A. Bernardini, J. O. Smith III, and A. Sarti, "An improved and generalized diode clipper model for wave digital filters," in *Proc. 139th Int. Audio Eng. Soc. (AES)*, New York, NY, Oct 29– Nov 11, 2015.

[32] A. Bernardini, K. J. Werner, A. Sarti, and J. O. Smith III, "Modeling nonlinear wave digital elements using the Lambert function," *IEEE Trans. Circuits Syst. I, Reg. Papers*, vol. 63, no. 8, Aug 2016.

[33] T. E. Rutt, "Vacuum tube triode nonlinearity as part of the electric guitar sound," in *Proc. 76th Int. Audio Eng. Soc. (AES)*, New York, NY, Oct 8–11, 1984.

[34] R. C. Smith, "Dual mode music instrument amplifier," U.S. Patent 4,211,893, issued Jul 8, 1980.

[35] K. J. Werner, W. R. Dunkel, and F. G. Germain, "A computational model of the Hammond organ vibrato/chorus using wave digital filters," in *Proc. 19th Int. Conf. on Digital Audio Effects (DAFx-16)*, Brno, Czech Republic, Sep 5–9, 2016.

[36] W. M. Leach Jr, "SPICE models for vacuum-tube amplifiers," *J. Audio Eng. Soc.*, vol. 43, no. 3, pp. 117–126, 1995.

[37] N. Koren, "Improved vacuum tube models for spice simulations," *Glass Audio*, vol. 8, no. 5, pp. 18–27, 1996.

[38] G. C. Cardarilli, M. Re, and L. Di Carlo, "Improved large-signal model for vacuum triodes," in *IEEE Int. Symp. Circuits Syst. (ICSCAS)*, Taipei, Taiwan, May 24–27, 2009.

[39] S. D'Angelo, J. Pakarinen, and V. Valimaki, "New family of wave-digital triode models," *IEEE Trans. Audio, Speech, Language Process.*, vol. 21, no. 2, pp. 313–321, Feb 2013.

[40] J. Mačák, J. Schimmel, and M. Holters, "Simulation of fender type guitar preamp using approximation and state space model," in *Proc. 15th Int. Conf. on Digital Audio Effects (DAFx-12)*, York, UK, Sep 17–21, 2012.

[41] P. Raffensperger, "Toward a wave digital filter model of the Fairchild 670 limiter," in *Proc. 15th Int. Conf. on Digital Audio Effects (DAFx-12)*, York, UK, Sep 17–21, 2012.

[42] K. Dempwolf and U. Zölzer, "A physically-motivated triode model for circuit simulations," in *Proc. 14th Int. Conf. on Digital Audio Effects (DAFx-11)*, Paris, France, Sep 19–23, 2011.

[43] C. Sanderson and R. Curtin, "Armadillo: a template-based C++ library for linear algebra," *J. Open Source Softw.*, vol. 1, pp. 26, 2016.

[44] S. Müller and P. Massarani, "Transfer-function measurement with sweeps," *J. Audio Eng. Soc.*, vol. 49, no. 6, pp. 443–471, 2001.

[45] M. Holters and U. Zölzer, "A k-d tree based solution cache for the non-linear equation of circuit simulations," in *Proc. 24th Eur. Signal Process. Conf. (EUSIPCO)*, Budapest, Hungary, Aug 29–Sep 2, 2016, pp. 1028–1032.